

## Supporting Information

# UV-weathering affects heteroaggregation and subsequent sedimentation of polystyrene microplastic particles with ferrihydrite

Johanna Schmidtman<sup>1\*</sup>, Hannah-Kristin Weishäupl<sup>1</sup>, Luisa Hopp<sup>1</sup>, Nora Meides<sup>2</sup>, Stefan Peiffer<sup>1</sup>

<sup>1</sup> Department of Hydrology, University of Bayreuth, Bayreuth Center for Ecology and Environmental Research (BayCEER), Bayreuth, Germany

<sup>2</sup> Department of Macromolecular Chemistry I, University of Bayreuth, Bayreuth, Germany

\* Corresponding author: [j.schmidtman@uni-bayreuth.de](mailto:j.schmidtman@uni-bayreuth.de)

## List of Tables

- Table S1.** Calculation of the total irradiance of the UV-weathering chamber and the acceleration factor for Germany.
- Table S2.** Application of the acceleration factor to the UV-weathering periods used in this study.

## List of Figures

- Figure S1.** Wavelength spectrum of a SOL500 lamp.
- Figure S2.** Images of the PS suspensions after different UV-weathering durations.
- Figure S3.** Simplified illustration of the sedimentation experiments with 10 mg L<sup>-1</sup> PS and 10 mg L<sup>-1</sup> ferrihydrite.
- Figure S4.** Zeta potential (**A**) and hydrodynamic diameter (**B**) of 10 mg L<sup>-1</sup> ferrihydrite.
- Figure S5.** SEM images of pristine PS particles.
- Figure S6.** SEM images of UV-weathered PS particles.
- Figure S7.** Sedimentation of (UV-weathered) PS in absence of ferrihydrite.
- Figure S8.** Conductivity of the initial 100 mg L<sup>-1</sup> PS suspensions after different UV weathering time steps.
- Figure S9.** Zeta Potential distribution of one single measurement of a sample with PS and ferrihydrite (pH 8.9) as an example for samples in which two zeta potential peaks were measured.
- Figure S10.** Zeta potential values and hydrodynamic diameter of samples with (UV-weathered) PS, ferrihydrite and PS + ferrihydrite compared for each weathering duration.
- Figure S11.** Illustration of interactions of weathered PS, Fh, and PS weathering products.

## List of Sections

- Section 1.** Additional experiments to analyze interactions between Fh and DOC components formed upon PS degradation.

**Table S1.** Calculation of the total irradiance of the UV-weathering chamber and the acceleration factor for Germany.

Solar irradiation per year (Germany)	1086 kWh m <sup>-2</sup>
Hours of solar irradiation per year	8760 h
Average solar irradiation intensity (Germany)	124 W m <sup>-2</sup>
Irradiation intensity UVACUBE + SOL500	1216.11 W m <sup>-2</sup>
<b>Acceleration factor</b>	<b>9.81</b>

For the calculation of the total irradiance of the PS particles in the weathering chamber, we used the global radiation in Germany (mean 30-year monthly and annual sums) as reference. For the period 1991-2020, the average radiation per year is 1086 kWh m<sup>-2</sup>.<sup>1</sup>

Compared to the average irradiation in Germany, the irradiance in the weathering chamber is approx. 10-fold enhanced.

**Table S2.** Application of the acceleration factor to the UV-weathering periods used in this study.

UV-weathering (hours)	Theoretical weathering time in Germany (days)
48	20
96	39
144	59
192	78
240	98
480	196
960	392

<sup>1</sup>[https://www.dwd.de/EN/ourservices/solarenergy/maps\\_globalradiation\\_mvs.html;jsessionid=1A740BA78B9C6A53FD423260F80C3EED.live11051?nn=495490](https://www.dwd.de/EN/ourservices/solarenergy/maps_globalradiation_mvs.html;jsessionid=1A740BA78B9C6A53FD423260F80C3EED.live11051?nn=495490), accessed 26.07.2023

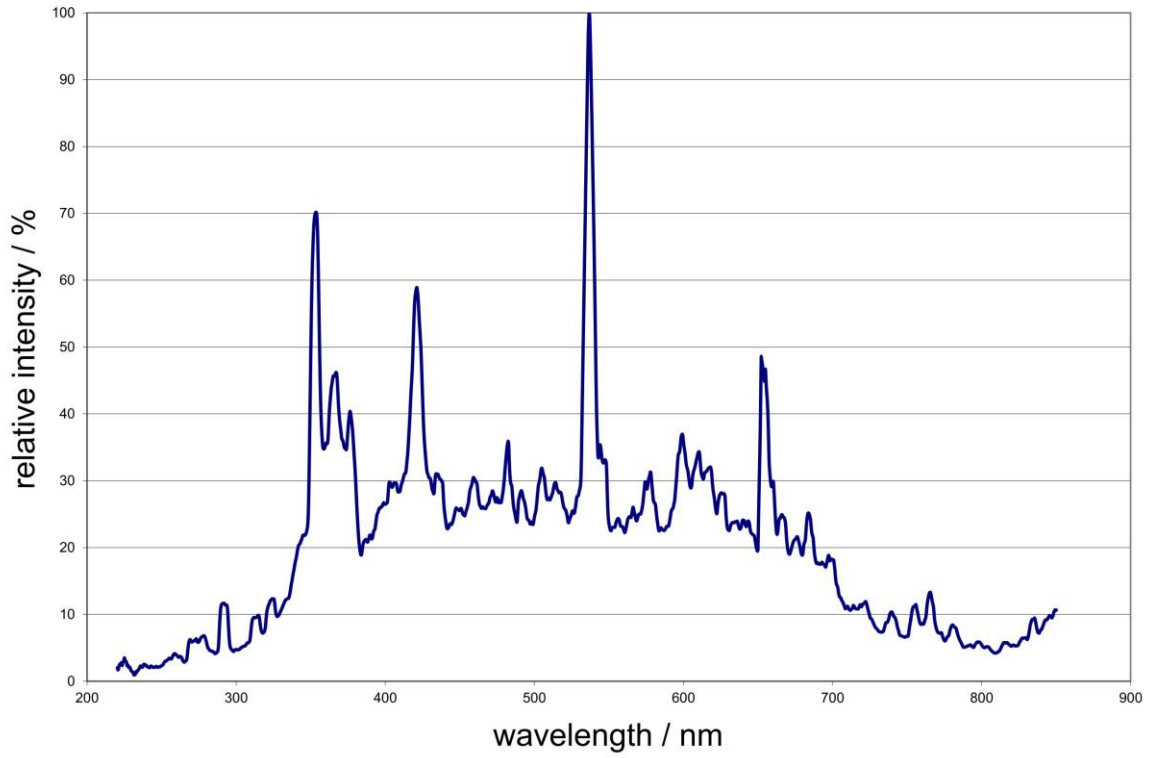


**Figure. S1.** Wavelength spectrum of a SOL500S lamp (without filterglass). The graph was provided by *Dr. Hönle AG*.

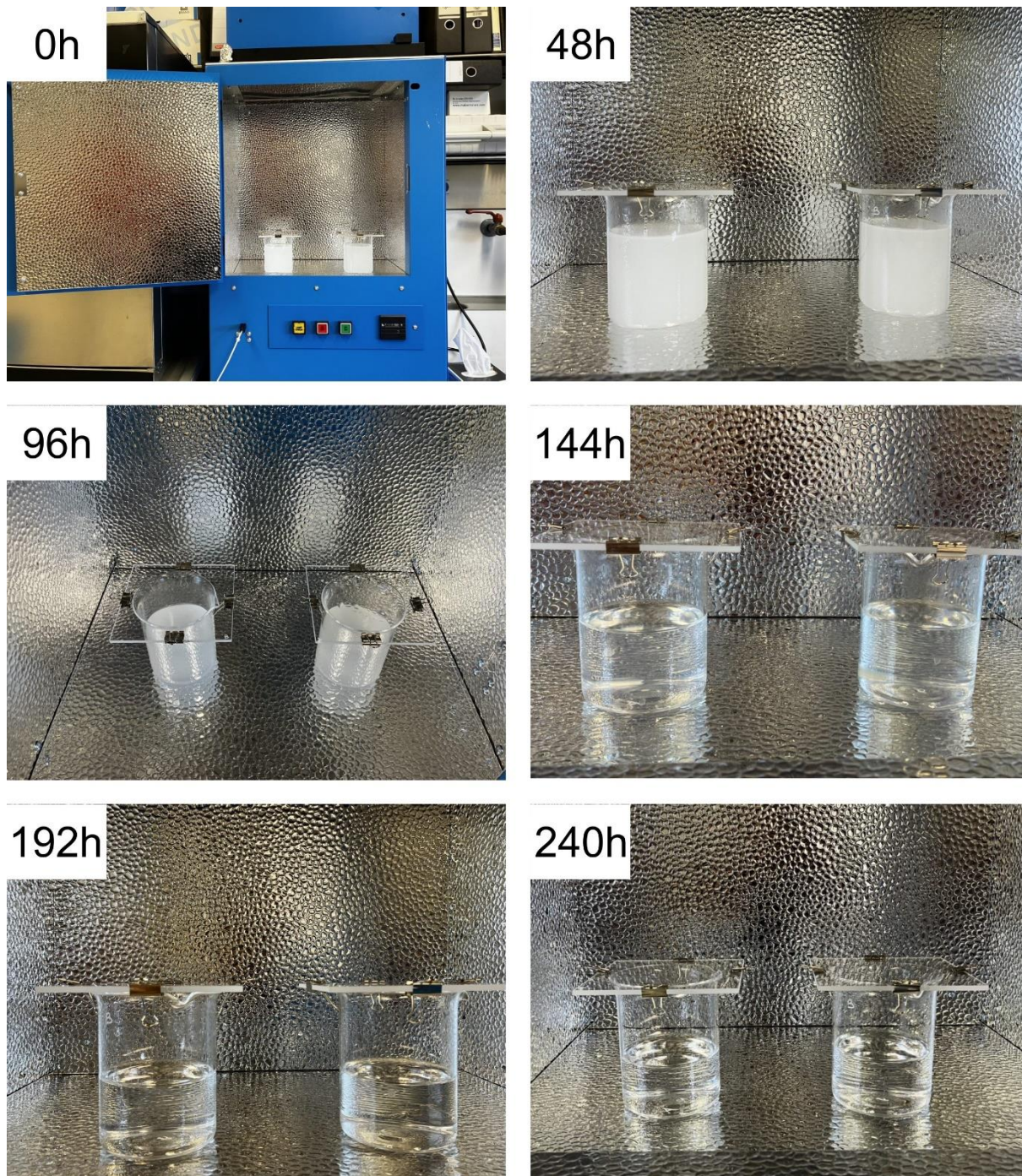


**Figure S2.** Images of the initial 100 mg L<sup>-1</sup> PS suspensions after different UV weathering durations in the weathering chamber.

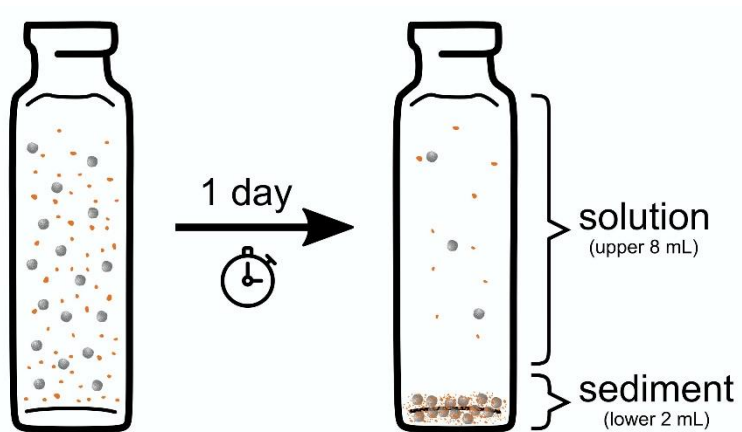


**Figure S3.** Simplified illustration of the sedimentation experiments with  $10 \text{ mg L}^{-1}$  PS and  $10 \text{ mg L}^{-1}$  ferrihydrite.

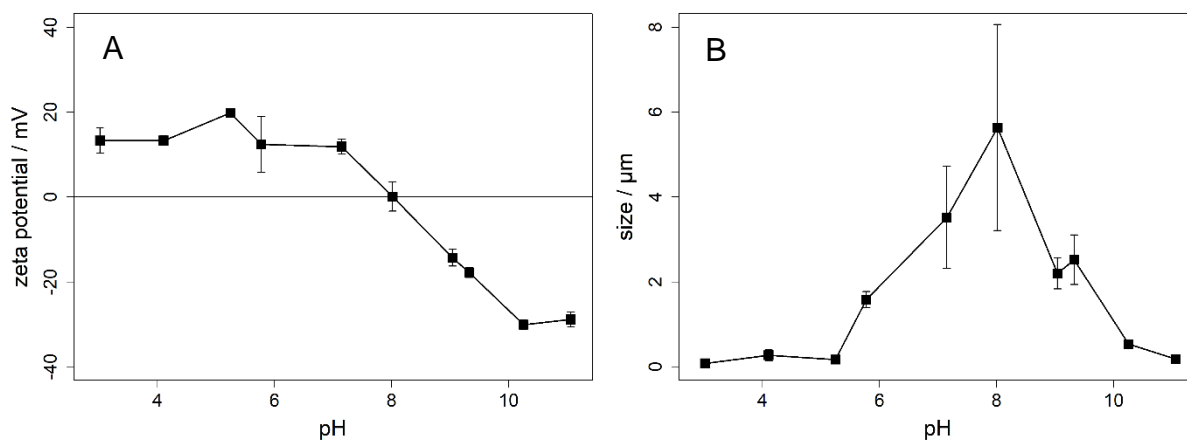


**Figure S4.** Zeta potential (A) and hydrodynamic diameter (B) of 10 mg L<sup>-1</sup> ferrihydrite. At acidic pH values, the particle size of ferrihydrite was only in nanometer size range and some of the material might have been present as dissolved iron. Therefore, the count rates of these samples might have been insufficient for reliable light scattering measurements.<sup>2</sup>

<sup>2</sup> Schmidtman et al., Environ. Sci.: Processes Impacts, 2022, 24, 1782–1789.

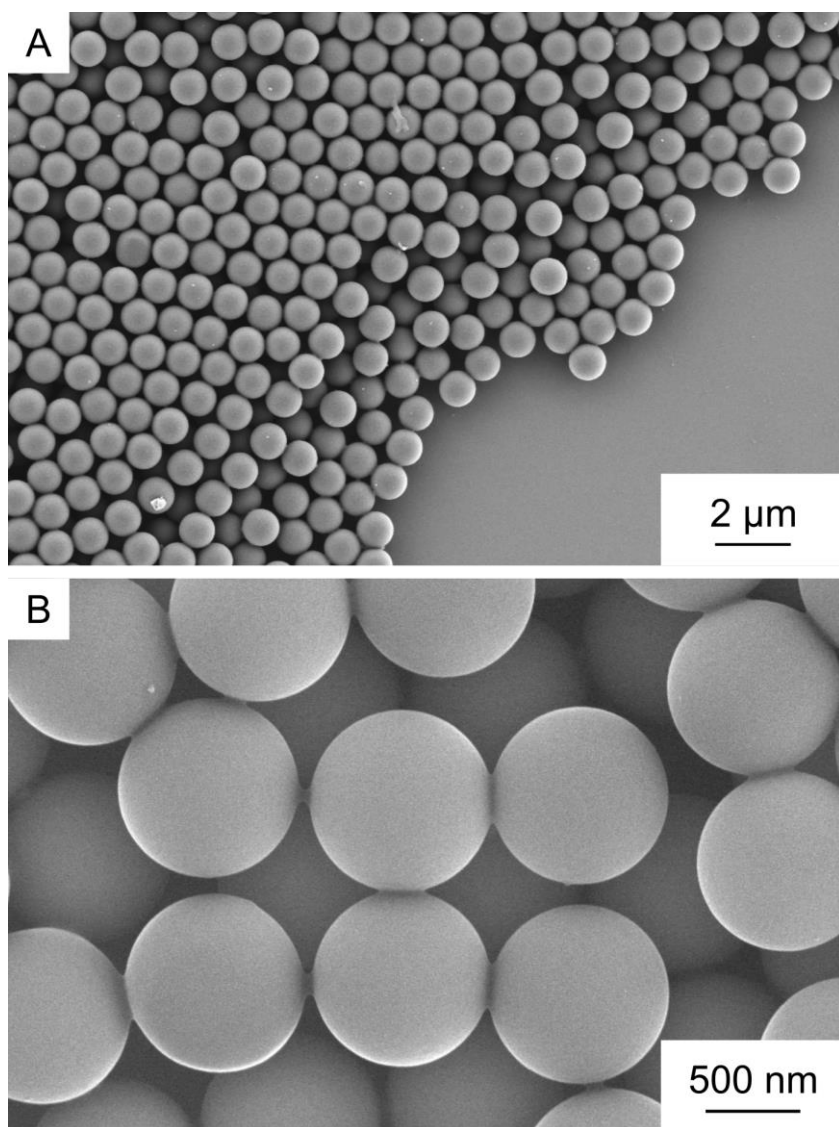


**Figure S5.** SEM images of pristine PS particles.

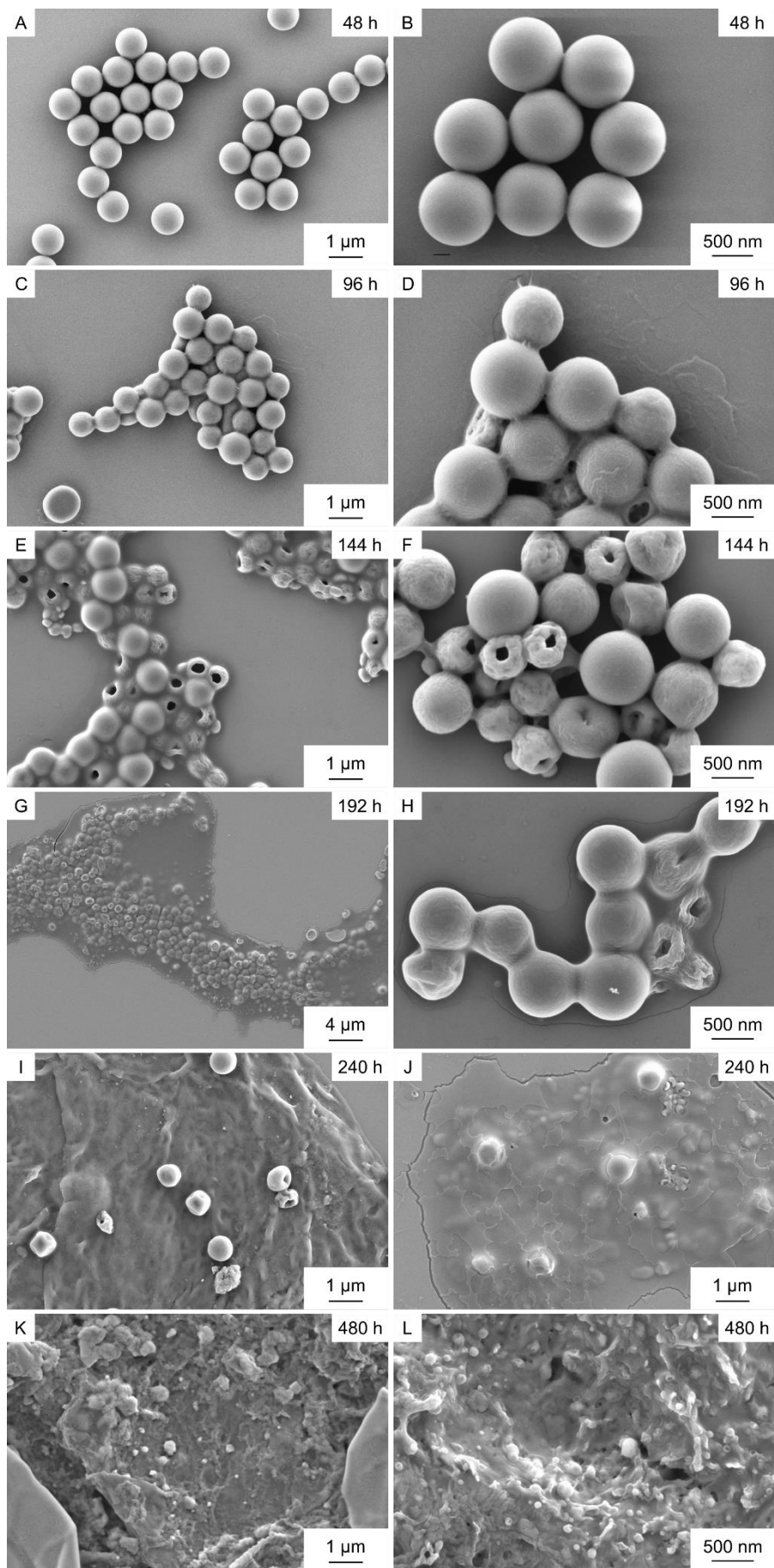


**Figure S6.** SEM images of UV-weathered PS particles.

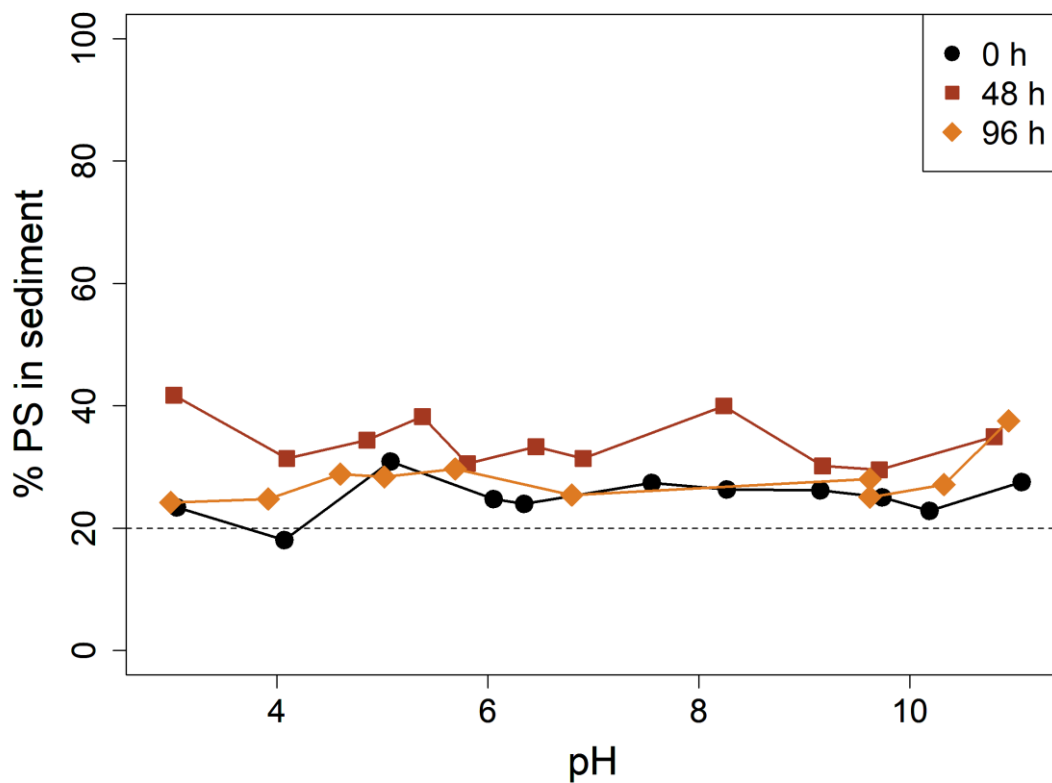


**Figure S7.** Sedimentation of pristine and UV-weathered PS in absence of ferrihydrite: Percentage of carbon found in the sediment after a settling time of one day. In a well-mixed dispersion where no sedimentation takes place, 20% of the total PS in the sample should be found in the sediment (dashed line).

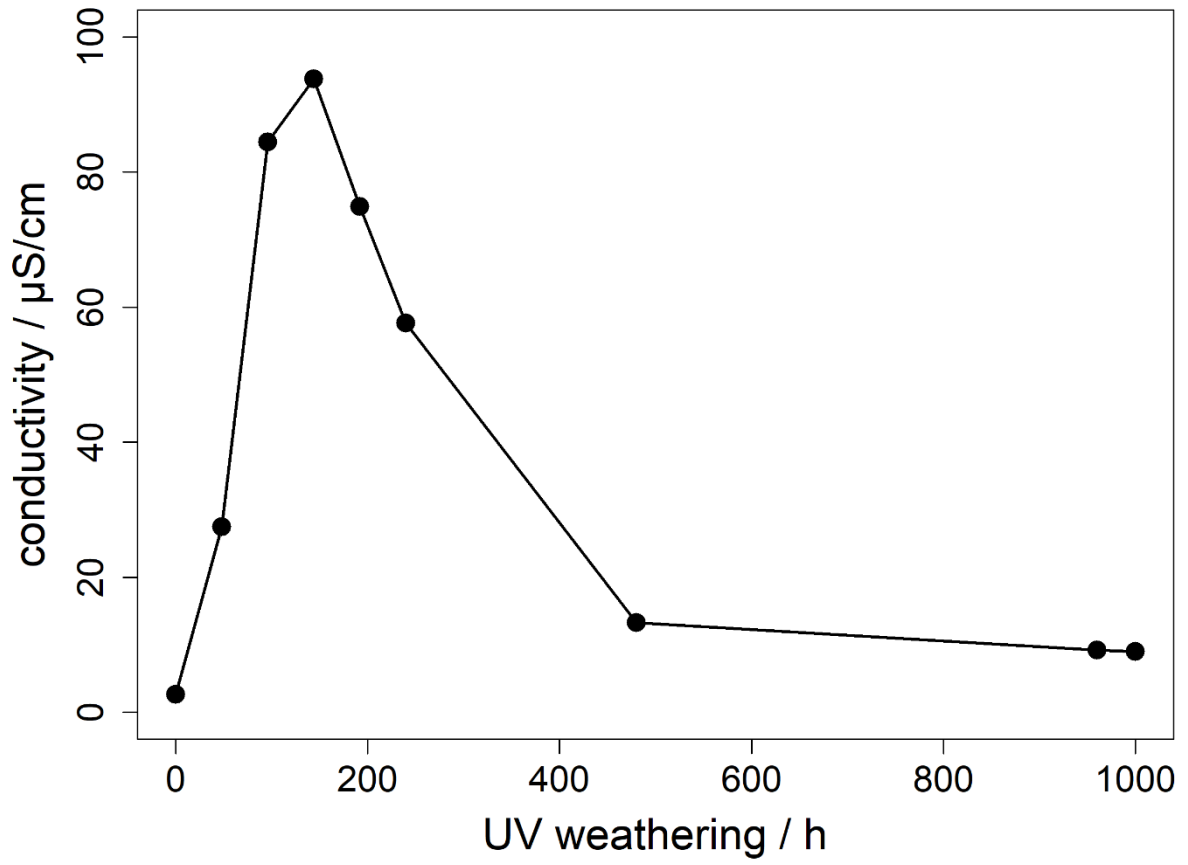


**Figure S8.** Electrical conductivity of the initial  $100 \text{ mg L}^{-1}$  PS suspensions after different UV-weathering time steps.

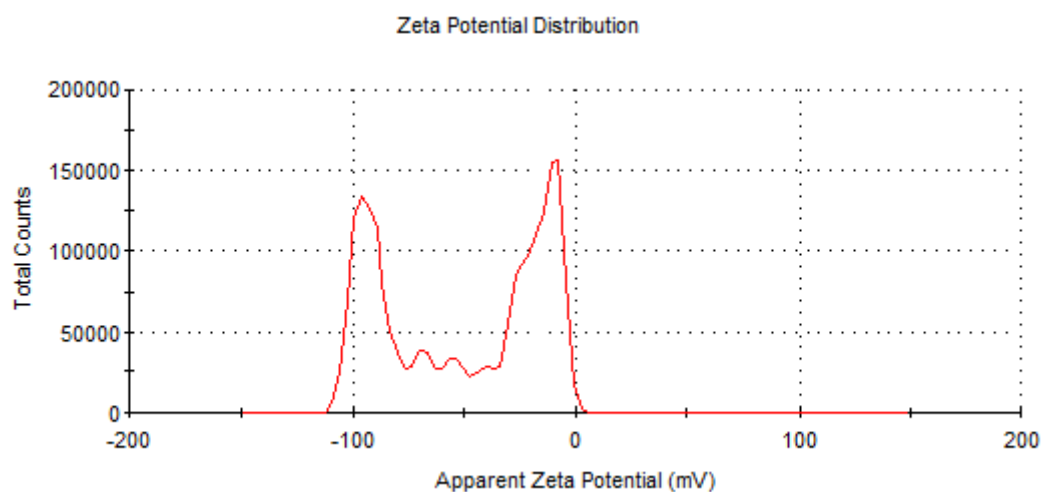


**Figure S9.** Zeta Potential distribution of one single measurement of a sample with PS and ferrihydrite (pH 8.9) as an example for samples in which two zeta potential peaks were measured. The zeta potential distributions do not show one but two distinct zeta potential peaks and therefore suggest the co-occurrence of PS and ferrihydrite particles that stay separated, and that no (major) aggregation takes place. The peak at -92 mV values can be attributed to the PS particles and the peak at -16 mV to the ferrihydrite particles.

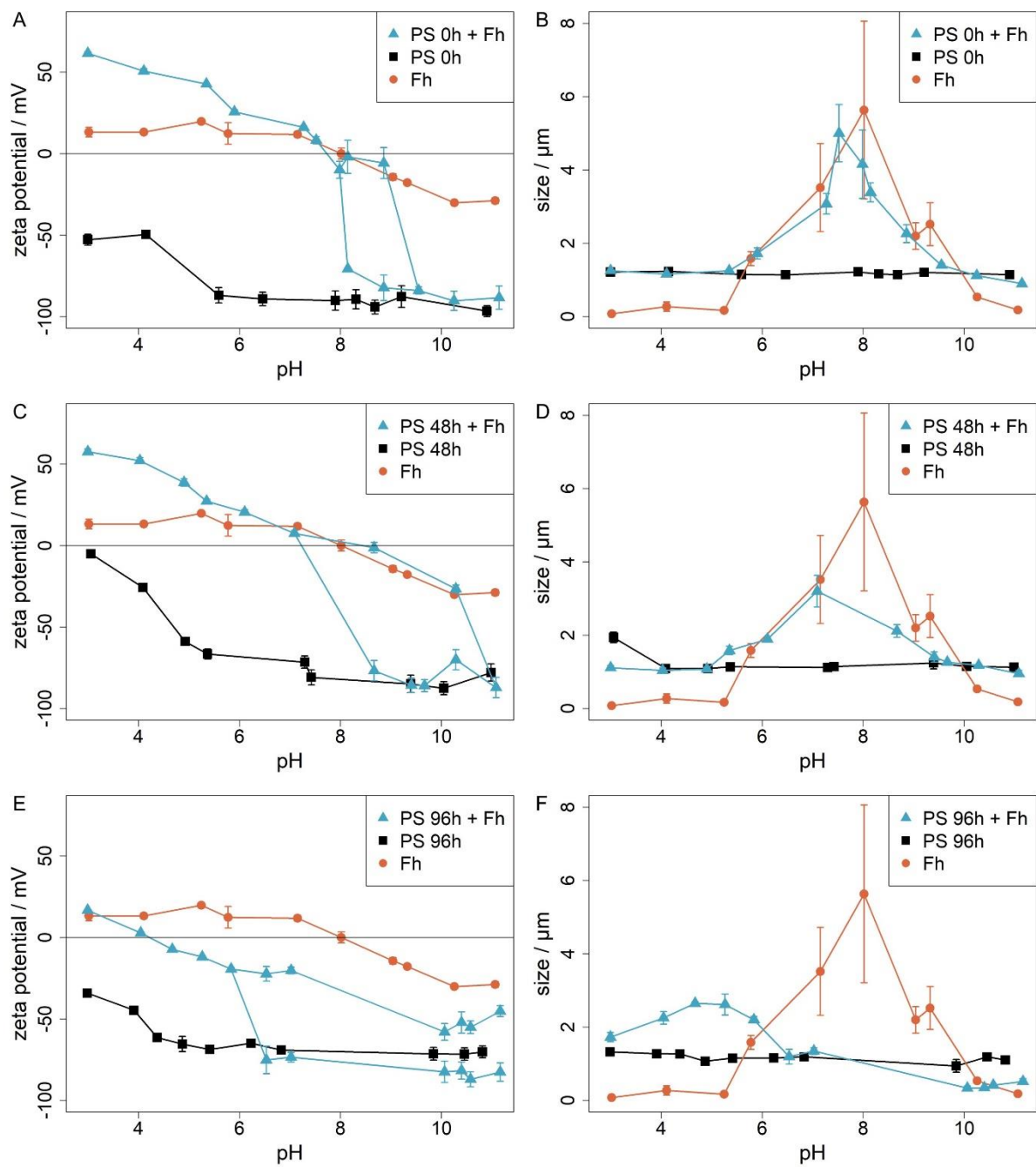


**Figure S10.** Zeta potential values and hydrodynamic diameter of samples with PS, ferrihydrite (Fh), and PS+Fh compared for each weathering duration (0, 48, and 96 h).

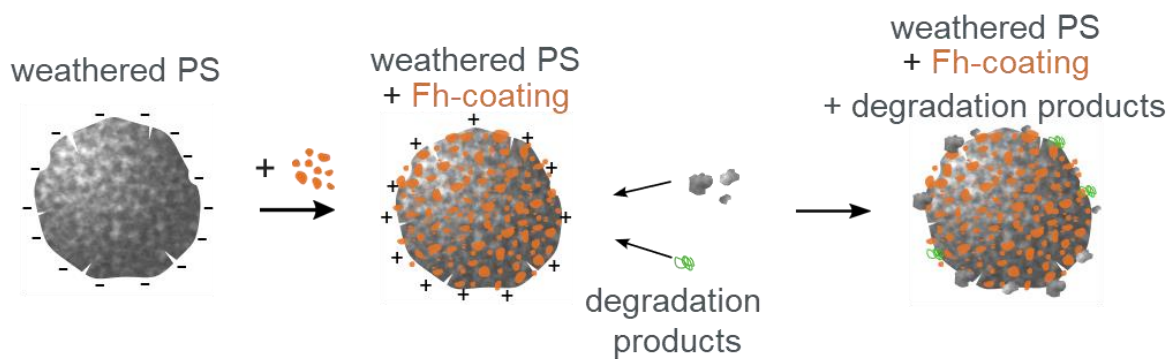


**Figure S11.** Illustration of interactions of weathered PS, Fh, and small PS weathering products at acidic pH values: In the first step, negatively charged PS<sub>96h</sub> particles that had been weathered only mildly, became coated with Fh. The now positively charged surfaces of these particles further interacted with the negatively charged smaller DOC components formed upon PS degradation, thereby reducing the net surface charge and allowing for aggregation.

## Section S1.

In order to test the hypothesis that not only PS particles (with altered properties due to weathering), but additionally, very small (filterable) particles and dissolved organic molecules, that have formed during weathering, may have interacted with Fh, we have performed additional experiments. For this end, we have filtered PS<sub>96h</sub> to remove the > 0.45 µm fraction and exposed the remaining MP-derived DOC to Fh.

### **Experimental setup**

Shortly, the additional experiments performed are described below:

- 1) Filtration of 100 mg/L PS<sub>96h</sub> suspension to obtain the < 0.45 µm fraction (filter: Chromafil Xtra PA-45/25, *Macherey-Nagel GmbH & Co. KG*, Germany). Further called: "DOC<sub>96h</sub>".  
Please note: Since the DOC fraction accounts for approximately 34% of the total carbon after 96 hours of weathering (Fig. 2), the DOC concentration in the filtered stock solution is accordingly around 34 mg/L. As the samples for sedimentation and ZetaSizer analysis, were prepared analogous to the experiments with the unfiltered suspension, the concentration of DOC in the samples was 3.4 mg/L.
- 2) Sedimentation analysis after 1 day reaction of (i) DOC<sub>96h</sub> only as a control and (ii) DOC<sub>96h</sub>+Fh was performed. The experimental procedure was done in analogy to the experiments with the unfiltered samples as described in section 2.3 and 2.4.1 in the manuscript
- 3) Zetapotential and hydrodynamic diameter analysis after 1 day reaction of (i) DOC<sub>96h</sub> only as a control and (ii) DOC<sub>96h</sub>+Fh were carried out. The experimental procedure was done in analogy to the experiments with the unfiltered samples as described in section 2.5 in the manuscript. Please note: The zeta potential and hydrodynamic diameter analysis of the control (DOC<sub>96h</sub> without Fh) did not generate qualitative acceptable results as the count rate was too low. This indicates that the remaining particles in the DOC<sub>96h</sub>-fraction were too small or even dissolved (as assumed in the manuscript) to generate reliable results using the ZetaSizer.

### **Results and Discussion**

The results of sedimentation experiments as well as zeta potential and hydrodynamic diameter analyses of DOC<sub>96h</sub> (in presence and absence of Fh) are presented in Fig. S12 (below). For better comparison, the results of the unfiltered PS samples are also presented in the same graphs (as indicated in the legends of the graphs).

Firstly, the results of sedimentation experiments (Fig. S12A) show that no major sedimentation is taking place after 1 day for DOC<sub>96h</sub>+Fh (C in sediment: 23.5% - 31.9%) or DOC<sub>96h</sub> alone (C in sediment: 22.7% and 24.9%). In a well-mixed dispersion, where no sedimentation takes place, 20% of the total C in the sample (dashed line) should be found in the sediment due to the experimental setup (Fig. S3).

Hydrodynamic diameter measurements revealed aggregate sizes between 0.14 – 1.1 µm (Fig. S12C) whereas the larger diameters were measured at smaller pH values. Zeta potential values were between -13.2 mV at pH 4.3 and -27.2 mV at pH 9.4 (Fig. S12B).

These results prove that Fh particles interacted with DOC<sub>96h</sub>, as indicated by the clear reduction in surface charge compared to Fh alone, particularly at acidic and neutral pH values. At acidic pH, these interactions likely facilitated the formation of Fh–DOC<sub>96h</sub> aggregates of approx. 1 µm in diameter. However, no substantial increase in sedimentation was observed, suggesting that the aggregates remained stable in suspension.

At neutral pH (7.6), the interaction with DOC<sub>96h</sub> led to a reduction in the surface charge of Fh, thereby increasing the repulsive forces between particles and preventing homoaggregation, as no increase in aggregate size was detected.

In conclusion, these additional experiments confirm that MP-derived DOC interacts with Fh, forming aggregates of up to 1  $\mu\text{m}$  in diameter with a negative net surface charge. These findings support our hypothesis that MP degradation products interact with Fh, resulting in a more complex system with distinct interaction dynamics. However, it is important to note that these additional experiments (of Fh and DOC<sub>96h</sub>) do not account for the combined effects of all species present in the original system, as the larger PS<sub>96h</sub> particles that had experienced only weak weathering effects were not included.

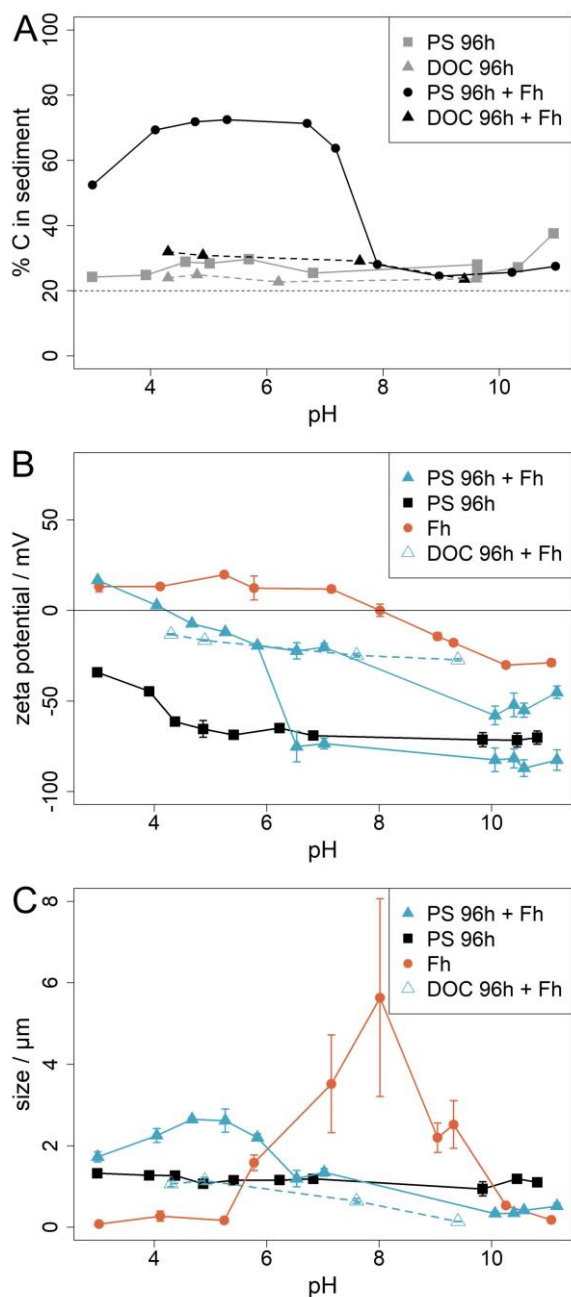


**Figure S12.** A) Sedimentation of PS<sub>96h</sub> and DOC<sub>96h</sub> in the presence and absence of Fh after a reaction time of 1 day. B) Zeta potential values and C) hydrodynamic diameter of samples containing PS<sub>96h</sub>, Fh, PS<sub>96h</sub>+Fh and DOC<sub>96h</sub>+Fh.